AIAA 82-4183

Correlation of Lift and Boundary-Layer Activity on an Oscillating Lifting Surface

Robert L. Bass,* James E. Johnson,† and James F. Unruh‡
Southwest Research Institute, San Antonio, Texas

Boundary-layer and trailing-edge flow activities were recorded using hydrogen bubble flow visualization techniques on an oscillating lifting surface in a two-dimensional water tunnel. Simultaneous with flow documentation, unsteady lift was measured over a range of reduced frequencies of 0.5-10. Unsteady loads using classical, inviscid theories were predicted for the experimental conditions investigated. Reduced frequency bands exhibiting poor agreement between experiment and theory were identified and a correlation to observed flow phenomena was accomplished. The results support the utilization of a separate viscous model near the trailing edge coupled with an inviscid flowfield model to predict unsteady loads. The results further show that for certain reduced frequency bands, classical inviscid solutions may be applicable and adequate.

Nomenclature

b = one-half chord length
c = chord length
$C(k)$ = Theodorsen function
$C_{L\alpha_0}$ = two-dimensional steady-state lift curve slope
$C_{L\tilde{\alpha}_{0s}}$ = oscillatory lift coefficient
f = oscillation frequency
k = reduced frequency ($\omega b/V$)
t = time
V = freestream velocity
X = distance along chord from leading edge
α = instantaneous angle of attack
$\tilde{\alpha}$ = oscillatory angle-of-attack amplitude
α_0 = mean angle of attack
δ = boundary-layer thickness
δ^* = boundary-layer displacement thickness
ΔW = width of lifting surface
ν = fluid kinematic viscosity
ω = circular frequency
ρ = fluid density
θ = phase shift in Theodorsen's function

Introduction

THE dynamics of the boundary layer (viscous effects) have an important bearing on lifting surface unsteady aero- and hydrodynamic behavior. Inviscid theories are not adequate in many practical applications in their prediction of unsteady loads or flutter inception.

Improved theories of lifting surface dynamic performance which account for real fluid effects are required to advance the state of unsteady aero- and hydrodynamics. This realization has led numerous researchers[1-9] to re-evaluate assumptions used in inviscid unsteady aerodynamic theories. Both analytical and experimental efforts have been undertaken. Most studies have evaluated the applicability of the Kutta condition in unsteady flows. Significant experimental activity has been undertaken to study trailing-edge loading and flow patterns on oscillating lifting surfaces. Theoretical efforts have also been initiated to include viscous corrections to inviscid solutions to allow better prediction of oscillatory loads. These research efforts have been accomplished primarily in 1974-1980. The following discussion is presented to summarize the current state of knowledge regarding oscillating load phenomena and to provide the basis for the results presented in this paper.

Gostelow[1] conducted an experimental study of trailing-edge flows over turbomachine blades. He showed that for most turbomachine blades with a rounded trailing edge, the Kutta condition has no meaning and that the effects of viscosity must be included in an unsteady flow environment to give a realistic prediction of blade loading. Gostelow concluded that until more reliable information is available on separation and transition behavior in unsteady and turbulent flows, any agreement between experiment and theory will continue to have an element of fortuity. Archibald[2] conducted an experimental study to evaluate the unsteady Kutta condition. Trailing-edge lift coefficients on a flat plate and an airfoil at high reduced frequencies were measured. For widely varying trailing-edge geometries, significant differences in the measured local lift coefficients C_L were recorded. Archibald concluded that for a turbulent boundary layer, the unsteady Kutta condition does not hold on a local basis; however, the integrated effect along the span would result in a nominally steady Kutta condition. Brown and Daniels[3] developed a theoretical model to account for viscous effects in the neighborhood of the trailing edge of an oscillating airfoil undergoing sinusoidal oscillations of high frequency and low amplitude. They divided the boundary layer above the plate into five distinct regions and developed asymptotic solutions in four of the regions and a linearized solution in the fifth region which yielded estimates for the viscous corrections to the circulation determined by the Kutta condition. No comparisons with experimental data were provided. Based on physical reasoning, Sears[4] concluded that the unsteady aerodynamics of airfoils with rounded trailing edges require a dual model involving the boundary-layer calculation over a smooth body to determine circulation and a vortex sheet model to determine the perturbed potential flowfield as well as the forces and moments on the airfoil.

Basu and Hancock[5] developed a numerical method for calculation of the pressure distributions, forces, and moments on a two-dimensional airfoil undergoing an arbitrary unsteady motion in an inviscid compressible flow. An excellent description of the applicability of the Kutta condition in oscillating flows was presented. A discussion of the appropriate Kutta condition was provided and it was argued that two Kutta conditions are required to obtain a satisfactory solution. The results were shown to be applicable for an

Received June 25, 1981; revision received Jan. 4, 1982.

*Director, Department of Mechanical Sciences.
†Manager, Department of Mechanical Sciences. Member AIAA.
‡Senior Research Engineer, Department of Engineering Mechanics. Member AIAA.

airfoil undergoing an arbitrary time-dependent motion if it is assumed that the flow remains attached and that it separates at the trailing edge of the airfoil. Daniels[6] extended the theoretical work[3] to include the matching of inviscid solutions to a consistent viscous flow structure at the trailing edge of an oscillating lifting surface.

Satyanarayana and Davis[7] conducted an experimental study of unsteady trailing-edge conditions. Their investigation was aimed at establishing the range of reduced frequencies over which the classical Kutta condition is valid and the nature of the deviation beyond this range. A wind-tunnel study using a NACA 64A010 airfoil was conducted and the trailing-edge loading was measured and compared with unsteady incompressible small-disturbance theory. It was concluded that the Kutta condition in the theoretical analysis is valid below a reduced frequency of about 0.6 in predicting the trailing-edge loading. At reduced frequencies greater than 0.8, the predicted results underestimate the measured loading and the deviations increase further with reduced frequency. Fleeter[8] conducted a study of trailing-edge conditions for unsteady flows at high reduced frequency. Trailing-edge pressure coefficients were measured in an attempt to determine the applicability of the Kutta condition for oscillating airfoils and cascades at high reduced frequencies. Time-variant surface pressure distributions in the trailing-edge region of an isolated flat plate, a flat-plate cascade, a cambered airfoil were measured. Data were correlated with an appropriate state-of-the-art zero incidence flat-plate theoretical model that applied the Kutta condition. The results indicated that at high reduced frequencies the Kutta condition is appropriate for a classical isolated flat plate and flat-plate cascade over a wide range of incidence angles. However, for the cambered airfoil cascade, the condition does not appear to be satisfied for any angle of incidence.

Yates[9] formulated a theory of oscillating thin airfoils in compressible viscous flow and applied it to the calculation of steady and unsteady loads on a family of symmetric Joukowski airfoils. The theory reduced to the form of an integral equation with a kernel function whose solution is obtained through a modal expansion technique taken from flat-plate thin airfoil theory. The effect of viscosity is to change the order of the singularity in the kernel function such that a unique solution is obtained for any cross-sectional geometry without using an auxiliary uniqueness criterion such as the Kutta condition or the principle of minimum singularity. The principal unsteady effect related to thickness is to introduce an explicit phase factor in the kernel function that is proportional to the time for vortex disturbances to be convected from the load point to the upwash point. It was concluded that viscous thin airfoil theory is a practical tool for introducing simultaneously the effects of viscosity and geometric thickness in two-dimensional unsteady aerodynamic theory.

In the composite, the above efforts represent both analytical and experimental research investigating the effects of viscosity on unsteady loads on oscillating lifting surfaces. The experimental efforts show that for many cases, viscous (real fluid) effects drastically alter the trailing-edge conditions on oscillating lifting surfaces and, thus, the classical Kutta condition is not maintained. The experimental work represents measurements of trailing-edge pressures and flowfield patterns under various oscillatory conditions. In some cases low reduced frequencies have been utilized and in other cases high reduced frequencies. Nearly all of the experimental data have been obtained in wind-tunnel studies on plates and airfoils in air. Theoretical work has replaced the Kutta condition with auxiliary conditions which appear appropriate relative to the viscous flow phenomena at the trailing edge and which alter the associated circulation.

The objective of this study is to expand the state of knowledge about the effects of unsteady boundary-layer activity (viscous effects) on the loads of oscillating lifting

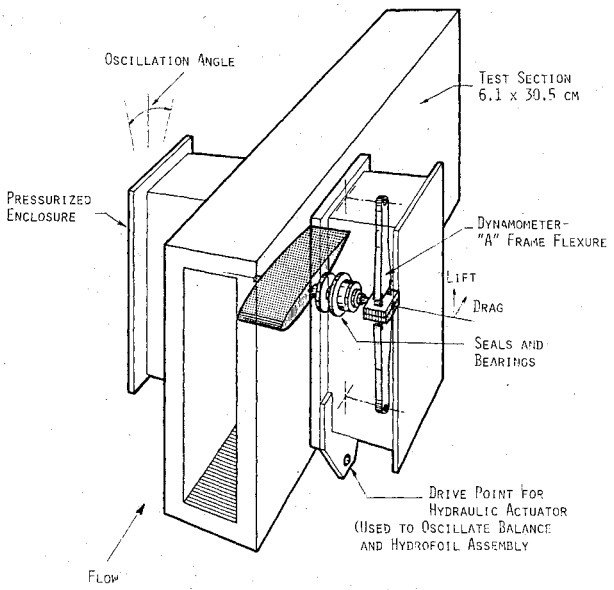

Fig. 1 Test section with balance and hydrofoil.

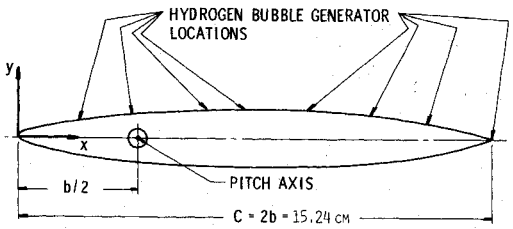

a) Model cross-section

SURFACE COORDINATES		BUBBLE GENERATOR
X (PERCENT C)	Y (PERCENT C)	LOCATION X_B (PERCENT C)
0	0	
1.25	1.292	
2.5	1.805	
5.0	2.509	
7.5	3.032	
10	3.457	12.9
15	4.135	
20	4.664	23.3
30	5.417	39.5
40	5.855	47.5
50	6.000	
60	5.835	61.4
70	5.259	74.3
80	4.199	36.0
90	2.517	
95	1.415	
100	0.120	100

LEADING EDGE RADIUS: 0.703 PERCENT C

b) Surface coordinates (NACA16-012)

Fig. 2 NACA 16-012 model surface and hydrogen bubble generator coordinates.

surfaces. These objectives were accomplished through visualizing the boundary-layer activity on a NACA 16-012 lifting surface harmonically pitching about the ¼ chord in a two-dimensional water tunnel. Simultaneously with boundary-layer observations and documentation, unsteady lift was measured for a wide range of reduced frequencies ($0.5 < k < 10$). The measurements were undertaken with the objectives of 1) evaluating the applicability of the Kutta condition over a wide range of reduced frequencies, and 2) establishing flow regimes where poor agreement exists between classical unsteady loads theory and experiment.

Experiments were undertaken in a two-dimensional water tunnel since higher Reynolds numbers could be achieved there than in a wind tunnel, and hydrogen bubble techniques could be utilized to visualize the unsteady boundary-layer activity. This work provides experimental data over a wider range of

reduced frequencies than previously available. It also represents data whereby total oscillatory lift was recorded simultaneously with the recording of unsteady boundary-layer activity.

Experimental Apparatus

Flow Tunnel and Instrumentation

Figure 1 shows the water tunnel test section used in this study. A rectangular two-dimensional test section of 6.1×30.5 cm provided a test section aspect ratio of 5. The test section length is 61 cm with a 45.7×30.5 cm high viewing area. A 1600 W quartz lamp placed over a plexiglass window 1.27 cm wide by 45.7 cm long located on the top surface provided light at 90 deg to the viewing angle and provided illumination for flow visualization. The water-tunnel test section shown in Fig. 1 was part of a continuous water-tunnel flow loop where 5.08 cm pipe was used for the return line. A 1.22 cm section of 35.6 cm pipe was placed upstream of the convergent section to form a stagnation chamber. A fixed-speed pump and throttling valve was used for flow control. Flow velocity was determined by measuring the time of a flight of a tracer along a known distance in addition to inferring average velocity from a 5.08 cm turbine flow meter.

Flow Visualization Equipment

Hydrogen bubbles were utilized to provide flow visualization for this study. A grid of platinum wire was placed upstream of the test model to provide visualization of the streamlines. In addition, hydrogen bubble generators were imbedded at different locations on the model surface to allow direct injection of tracers into the oscillating foil boundary layer. Photography of the hydrogen bubble tracers was successfully accomplished with a 16 mm high-speed motion picture camera with a zoom lens. The water-tunnel test section viewing window was marked with a vertical line for a tracer reference point. The developed film was analyzed frame by frame on a Vanguard motion analyzer where flight trajectories of hydrogen bubbles were easily determined. The film analyzer was configured to computerize the coordinates of motion of the flow tracers. The computerized space-time histories of individual bubbles were used to establish flow separation and reattachment locations and reverse flow activity during a foil oscillation cycle. These data were used for recording qualitative information on boundary-layer activity and were not used for load determination.

Dynamometer Design

A dynamometer, based upon the work of Epperson and Pengelley,[10] was used for measuring the dynamic lift coefficient on the oscillating model. The dynamometer, shown in Fig. 1, is classified as an external dynamic balance which can resolve two forces (vertical and horizontal) and one moment about a given axis perpendicular to the plane containing the two forces. Electric resistance strain gages attached to the structural elements of the A-frame flexures mounted back-to-back were incorporated in a Wheatstone bridge circuit in such a manner that the bridge output was proportional to the applied external moment or load.

The airfoil section was supported by a shaft connected to an external dynamometer unit located on each side of the tunnel test section. The dynamometer units were attached to a clevis that was allowed to rotate upon shaft bearings mounted on the tunnel side walls. Oscillatory motion was imparted by a hydraulic servocylinder located on the lower structure of the test section. A unique pressure balanced seal was fabricated which absorbs no load but inhibits the flow of liquid from the test section to the surroundings.

Model Design

A NACA 16-012 airfoil section molded of Resolin compound in two halves with a chord 15.2 cm long was used for the model. An oscillation shaft was positioned at the quarter-chord point. The shaft was hollow and carried electrical wires from the surface hydrogen bubble generators to the power source. Surface generators were made of gold-plated aluminum chips, $0.159 \text{ cm} \times 0.635$ cm imbedded flush in the surface of the hydrofoil. Figure 2 shows the model cross section with the bubble generator locations and surface coordinates.

Flow Visualization Results

Table 1 summarizes the test conditions investigated. Flow visualization was obtained while varying four parameters: freestream velocity, oscillation frequency, mean angle of attack, and pitch amplitude. In each test set (Table 1), one parameter was varied with the others held constant. For the velocity and frequency variation test, the mean angle of attack was held at approximately 5.8 deg with a pitch amplitude of ± 1 deg. Using 5.8 deg for the mean angle of attack allowed a sufficient boundary-layer growth to be observed during a full oscillation cycle while maintaining a relatively small angle of attack. All oscillatory tests were performed with harmonic pitching about the ¼ chord.

Initial tests were performed without oscillation to visualize and record steady-state boundary-layer activity as a function of angle of attack. The results showed that the boundary layer separated at $X/2b = 0.88$, 0.84, and 0.75 for $\alpha = 1.4$, 2.1, and 5.1 deg, respectively. This separation near the trailing-edge results from the rapid change in slope of the foil surface at $X/2b \geq 0.75$. Aerodynamic C_L data for this profile (NACA 16-012) indicate that the stall angle of attack occurs at $\alpha_s = 8$ deg. With the exception of test runs $H\alpha_0$-3 and $H\alpha$-3a, all test cases were performed with maximum angle of attack below the stall angle.

The flow visualization studies revealed that boundary-layer activity varied significantly depending on reduced frequency k. In general, a more pronounced degree of boundary-layer activity and instability was observed at $k < 1$. At all test conditions for $1 < k < 10$ reduced boundary-layer activity was observed, and at $k > 10$ a distinct boundary layer and wake flow regime developed. Table 2 summarizes the important boundary-layer observations for the test conditions of major interest. Figure 3 shows trailing-edge flow patterns during a pitch oscillation cycle at $k = 0.81$. This general trailing-edge flow activity was observed at all test cases with $k < 10$. Figure 4 shows instantaneous trailing-edge flow patterns from the movie frames for $k < 10$ and > 10. A description of the boundary-layer activity as a function of reduced frequency follows:

1) At the lowest frequency tested ($k = 0.45$), the boundary layer remained attached to the foil until approximately the ¾

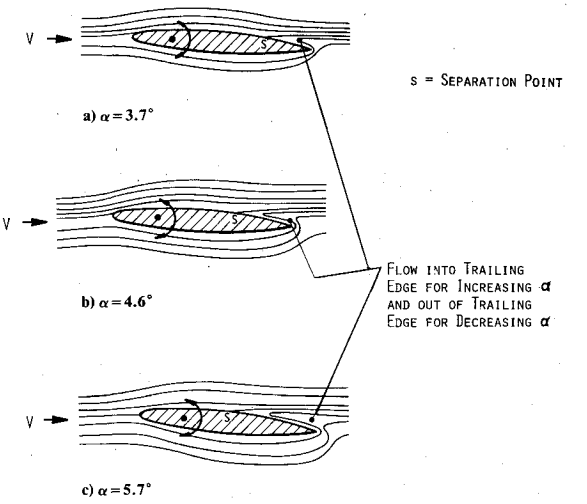

Fig. 3 Trailing-edge flow patterns ($k = 0.81$) at discrete α.

Table 1 Model test conditions

Run	Freestream velocity, V, cm/s	Oscillation frequency, f, Hz	Reduced frequency, $k=2\pi fb/V$	Reduced velocity, $1/k$	Angle of attack, deg $\alpha(t)=\alpha_0+\bar{\alpha}\sin 2\pi ft$	Reynolds No.,[a] $Re=2Vb/\nu$	$Re^*=V\delta^*/\nu$
				1) Velocity variation			
HV-1	9.82	0.132	0.648	1.54	$5.85+0.95\sin 0.83t$	16,105	219
HV-2	3.90	0.147	1.80	1.55	$5.825+1.025\sin 0.925t$	6,390	138
HV-3	16.23	0.151	0.445	2.25	$5.775+1.025\sin 0.947t$	26,620	282
HV-4	12.51	0.144	0.552	1.81	$5.80+1.0\sin 0.905t$	20,650	247
				2) Frequency variation			
HW-1	4.33	0.387	4.28	0.234	$5.9+0.9\sin 2.43t$	7,105	146
HW-2	4.18	0.329	3.76	0.266	$6.05+0.95\sin 2.07t$	6,865	143
HW-3	4.07	0.836	9.84	0.102	$6.05+0.95\sin 5.26t$	6,70	141
HW-4	3.69	0.241	3.13	0.319	$6.05+0.95\sin 1.51t$	6,060	135
				3) Mean angle-of-attack variation			
Hα_0-1	3.99	0.436	5.24	0.191	$1.95+1.05\sin 2.74t$	6,545	140
Hα_0-2	4.18	0.602	6.89	0.145	$5.60+1\sin 3.78t$	6,860	143
Hα_0-3	4.56	0.575	6.04	0.166	$7.65+1.15\sin 3.61t$	7,485	150
Hα_0-4	4.34	0.633	6.98	0.143	$-1.55+1.05\sin 3.98t$	7,125	146
Hα_0-5	4.50	0.649	6.90	0.145	$-5.25+1.05\sin 4.08t$	7,385	149
				4) Pitch amplitude variation			
H$\bar{\alpha}$-1a	5.89	0.503	4.09	0.244	$4.25+1.55\sin 3.16t$	9,655	170
H$\bar{\alpha}$-2a	5.76	0.47	3.91	0.256	$4.25+2.45\sin 2.95t$	9,450	168
H$\bar{\alpha}$-3a	5.78	0.446	3.69	0.271	$4.20+4.8\sin 2.80t$	9,475	168

[a] δ^* – based on theoretical value for an equivalent flat plate of chord $2b$.

Table 2 Model boundary-layer observations

Flow regime ident.	Run	K	$1/k$	V, cm/s	f, Hz	Observed boundary-layer activity[a]
A	HV-3	0.45	2.2	16.2	0.15	BL separation at $X/2b\cong 0.75$ Fluid flows into separation zone at TE at $\alpha_{max}=6.8$ deg Fluid pumped out of separation zone at TE at $\alpha_{min}=4.8$ deg
	HV-4	0.55	1.8	12.5	0.14	LE separation at $X/2b\cong 0.17$ Reattached BL at $X/2b\cong 0.4$ TE separation at $X/2b\cong 0.56$ Separation zone activity similar to HV-3
B	HV-1	0.65	1.5	9.8	0.13	LE separation at $X/b\cong 0.125$ with slight oscillation of separation point during foil pitching cycle Reattached BL at $X/2b\cong 0.48$ TE separation at $0.625\lesssim X/2b\lesssim 0.77$ (TE separation zone oscillates during foil cycle)
C	HW-1a	0.81	1.2	8.5	0.15	On verge of LE separation at $X/2b\cong 0.18$ TE separation at $0.5\lesssim X/2b\lesssim 0.75$ (TE separation zone oscillates during foil cycle)
D	HV-2	1.8	0.56	4.0	0.15	BL separation at $X/2b\cong 0.25$ (reverse flow oscillates in separation zone during foil cycle)
E	HW-4	3.1	0.32	3.7	0.24	
	HW-2	3.8	0.26	4.3	0.33	Identical to HV-2
	HW-1	4.3	0.73	4.3	0.39	
	HW-3	9.8	0.10	4.0	0.84	
F	—	10.9	0.09	4.9	1.10	Vortex shedding at TE at $k>10$

[a] Nomenclature: BL = boundary layer, TE = trailing edge, LE = leading edge, and b = semichord ($c/2$).

chord where the boundary layer separated from the foil surface. During an oscillation cycle fluid was pumped into the separation zone along the foil trailing edge as the angle of attack increased to the maximum value of 6.8 deg. As the foil reversed direction and proceeded to lower angles of attack, fluid was pumped out of the separation zone into the wake until the minimum angle of attack of 4.8 deg was reached.

2) Increasing reduced frequency to $k=0.55$ resulted in leading-edge separation at $X/2b=0.17$. The boundary layer reattached at approximately 40% of the chord and separated again at about 56% of the chord. Activity in the separation zone at the trailing edge of the foil was similar to the $k=0.45$ case.

3) Increasing k to 0.65 resulted in leading-edge separation at $X/B\cong 0.125$ with a slight oscillation of the leading-edge separation point during a foil pitching cycle. The boundary layer reattached at approximately 50% of the chord with reseparation oscillating between $0.625<X/2b<0.77$ during a pitch oscillation cycle.

4) Increasing k to 0.81 resulted in near elimination of leading-edge separation. For this case it appeared that leading-edge separation was on the verge of occurring at $X/2b=0.18$, although no distinct leading-edge separation could be discerned. Trailing-edge separation occurred between the 50 and 75% chords with the separation location oscillating during a foil oscillation cycle.

5) Increasing k to 1.8, and at all higher values up to $k=10$, resulted in the boundary layer separating at approximately the ¼ chord as compared to separation at $\sim 0.75X/2b$ for steady-state flow at an equivalent $\bar{\alpha}$.

6) At $k\geq 10$ a distinct vortex shedding from the foil trailing edge was observed, with the vortex shedding frequency equal to the pitch oscillation frequency.

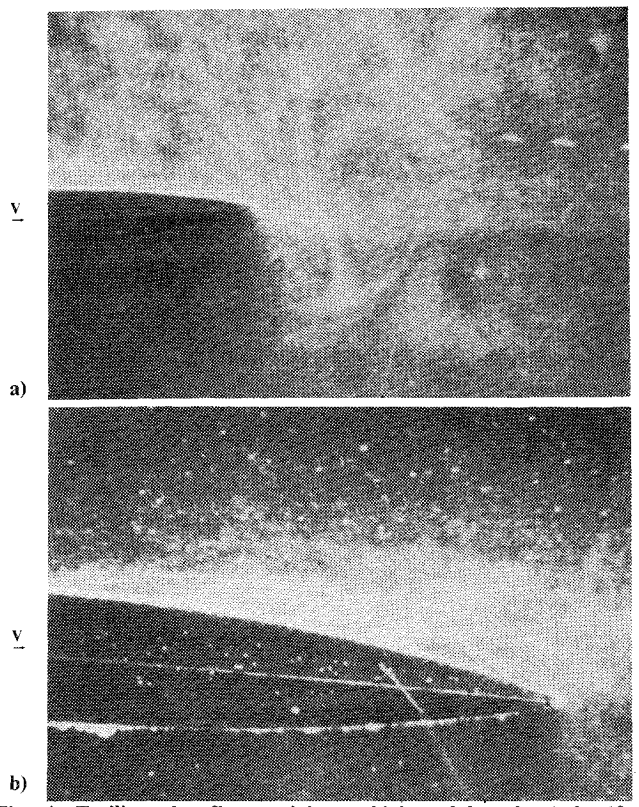

Fig. 4 Trailing-edge flow activity at high and low k: a) $k>10$, b) $k<10$.

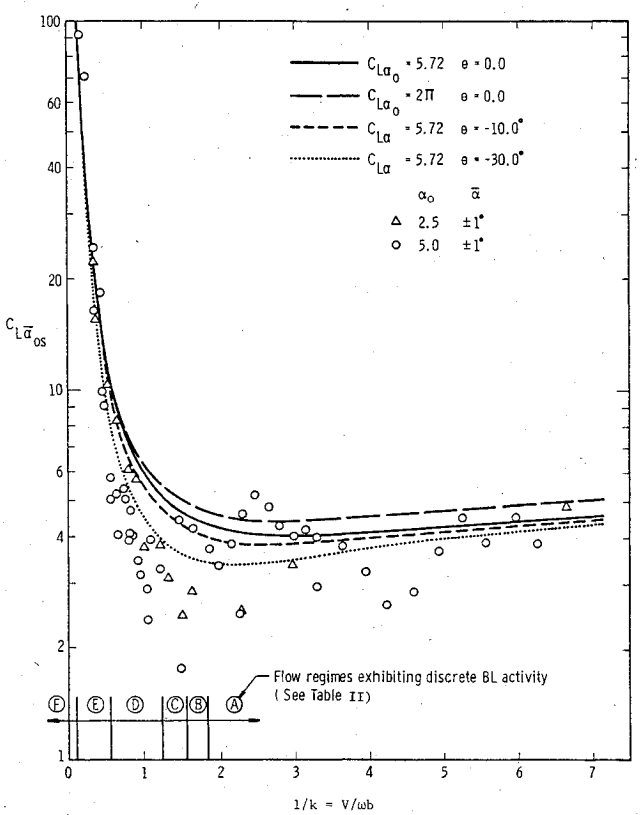

Fig. 5 Comparison of theory and experiment for oscillatory lift coefficient $C_{L\bar{\alpha}_{0s}}$ vs $1/k$.

7) During an oscillation cycle, flow activity in the separation region for any k value was identical to that described for $k=0.45$. Increasing mean foil angle of attack resulted in a wider separation region and more pronounced activity in the separation zone.

The observed boundary-layer activity on the oscillating model is noteworthy in the region of reduced frequencies between 0.8 and 1.8. Data in Ref. 11 indicates that experimental unsteady load data on hydrofoils are in poor agreement with theory for $k>1$. The flow visualization results indicate a transition in boundary-layer behavior in this region. In addition, the results of the flow visualization studies presented above reveal that the Kutta condition appears to be violated, with the flow phenomena at the trailing edge being dependent on k. This observation implies that relaxing the Kutta condition is a valid approach to providing more realistic predictions of hydrofoil performance. Also, the unstable boundary-layer activity observed at k values <1 implies that incorporating boundary-layer stability theory in a hydrofoil loads analysis should be a reasonable approach to improving current theoretical methods.

Correlation of Loads to Observed Boundary-Layer Activity

Simultaneous with boundary-layer documentation, unsteady lift measurements were made. Figure 5 shows a comparison of theory and experiment for oscillatory lift coefficients $C_{L\bar{\alpha}_{0s}}$ vs reduced velocity ($1/k$). Also shown on this figure are the various flow regimes (see Table 2) where different distinct boundary-layer activity was observed during the flow visualization.

Theoretical oscillatory lift coefficients were predicted using the classical predictions of Theodorsen[12] and the modified strip theory approach of Yates[13] wherein the actual two-dimensional lift curve slope for the experimental model ($C_{L\alpha_0}=5.72$/rad) was employed. The measured steady-state two-dimensional lift curve slope of 5.72/rad is in good agreement with the expected value for thick sections.[14] The oscillatory lift coefficient (for pitch about the ¼ chord) as a function of reduced frequency is given by

$$C_{L\bar{\alpha}_{0s}}=\left\{\pi\left[ik-\frac{k^2}{2}\right]+C_{L\alpha_0}C(k)\,[1+ik]\right\} \tag{1}$$

where $C_{L\bar{\alpha}_{0s}}$ is defined as

$$C_{L\bar{\alpha}_{0s}}=\frac{L}{\frac{1}{2}\rho V^2\Delta W 2b\bar{\alpha}e^{i\omega t}} \tag{2}$$

and L is the total lift force, ΔW the section width, and $C(k)$ the Theodorsen function. With phase shift θ the circulation function $C(k)$ appears as

$$C(k)'=C(k)e^{i\theta} \tag{3}$$

A phase shift between the virtual mass and oscillatory lift contributions to $C_{L\bar{\alpha}_{0s}}$ was introduced to synthesize changes in the Kutta condition.

From the data shown in Fig. 5, it can be seen that agreement between theory and experiment is good in those regions where boundary-layer activity is well behaved. For $1/k<0.75$ ($k>1.33$) good agreement between theory and experiment is noted; and for $1/k>2$ ($k<0.5$) reasonable agreement is noted. However, at the knee of the theoretical curves ($0.75<1/k<2.0$), significant deviation between measured and predicted oscillatory lift coefficient is noted. This flow regime represents conditions where the greatest degree of boundary-layer activity is recorded, wherein significant separation and reattachment of the boundary layer was observed. Also, the flow near the trailing edge was separated with flow alternating around the trailing-edge region as the foil oscillated through its maximum and minimum angle of incidence. Since such trailing-edge flow

conditions significantly affect the circulation around the oscillating foil in comparison to that predicted from classical inviscid theory, lift predictions were also carried out for various values of θ. As noted in Fig. 5, a 30 deg phase lag in $C(k)$ provides improved agreement between theory and experiment.

Conclusion and Recommendations

The presented simultaneous unsteady loads measurements and boundary-layer flow visualization provide additional insight into the effects of viscosity on unsteady loads on oscillating lifting surfaces, and additional insight into the flow conditions which occur in different reduced frequency bands. The results in this paper show that:

1) The Kutta condition, based on qualitative flow visualization, was violated for many of the observed oscillating foil test conditions.

2) Observed boundary-layer phenomena support the hypothesis that unsteady boundary-layer activity is responsible for the poor agreement between current theoretical predictions and experimental data used for predicting hydrofoil unsteady loads and flutter.

3) The largest disagreement between unsteady load theory and experiment occurs in the reduced frequency range, $0.5 \leq 1/k \leq 2$, which corresponds with the most pronounced boundary-layer activity (i.e., flow separation, flow around the trailing edge, etc.).

4) Introducing a phase lag into the circulation function provides better agreement between theory and experiment.

The experimental work presented in this paper supports the utilization of a separate viscous model in the trailing edge of an oscillating lifting surface which can be coupled with an inviscid flowfield model to provide unsteady load predictions. The results of this study should be compared to the analytical predictions of Refs. 6 and 9. The results further show that for certain reduced frequency bands classical inviscid solutions may be applicable and adequate.

Acknowledgments

The authors of this paper wish to express their appreciation to Dr. H. Norman Abramson who first suggested this work. Also, we want to express our gratitude to C. M. Wood for his dedicated work in conducting the experiments, Victoriano Hernandez for his skillful artwork on the figures, and Adeline K. Raeke for typing the text.

References

[1] Gostelow, J. P., "Trailing Edge Flows Over Turbomachine Blades and the Kutta-Joukowski Condition," ASME Paper 75-GT-94, Dec. 1974.

[2] Archibald, F. S., "Unsteady Kutta Condition at High Values of the Reduced Frequency Parameter," *Journal of Aircraft,* Vol. 12, June 1975, pp. 545-550.

[3] Brown, S. N. and Daniels, P. G., "On the Viscous Flow About the Trailing Edge of a Rapidly Oscillating Plate," *Journal of Fluid Mechanics,* Vol. 67, Pt. 4, 1975, pp. 743-761.

[4] Sears, W. R., "Unsteady Motion of Airfoils with Boundary-Layer Separation," *AIAA Journal,* Vol. 14, Feb. 1976, pp. 216-220.

[5] Basu, B. C. and Hancock, G. J., "The Unsteady Motion of a Two-Dimensional Aerofoil in Incompressible Inviscid Flow," *Journal of Fluid Mechanics,* Vol. 87, Pt. 1, 1978, pp. 159-178.

[6] Daniels, P. G., "On the Unsteady Kutta Condition," *Quarterly Journal of Mechanics and Applied Mathematics,* Vol. XXXI, Pt. 1, Feb. 1978, pp. 49-75.

[7] Satyanarayana, B. and Davis, S., "Experimental Studies of Unsteady Trailing-Edge Conditions," *AIAA Journal,* Vol. 16, Feb. 1978, pp. 125-129.

[8] Fleeter, S., "Trailing Edge Conditions for Unsteady Flows at High Reduced Frequency," *AIAA Journal,* Vol. 18, May 1980, pp. 497-503.

[9] Yates, J. E., "Viscous Thin Airfoil Theory," ARAP Rept. 413, Contract N00014-77-C-0616, Feb. 1980.

[10] Epperson, T. B. and Pengelley, C. D., "An Electric Resistance Type, Inertia-Cancelling, Dynamic Load Measuring Device," U. S. Air Force Contract AF 33 (616)-176.

[11] Abramson, H. N., Chu, W.-H., and Irick, J. T., "Hydroelasticity," Contract Nonr-4830(00)(X), Aug. 1966.

[12] Theodorsen, T., "General Theory of Aerodynamic Instability and the Mechanism of Flutter," NACA Rept. 496, 1935.

[13] Yates, E. C. Jr., "A Modified-Strip-Analysis Method for Predicting Wing Flutter at Subsonic to Hypersonic Speeds," N66-36094 (NASA TM-X-54830, 1964).

[14] Abbott, I. H. and Von Doenhoff, A. E., *Theory of Wing Sections,* Dover Publications, New York, 1959.